



Accepted: 21th July, 2024

Published: 29th August, 2024

1. Department of Chemistry, Federal University Lokoja, Kogi State

2. Department of Chemistry, Federal University Dutsin-Ma, Dutsin-Ma, Katsina State

*Corresponding Author:

Dr. Siaka Abdulfatai

f.isiaka@fudutsinma.edu.ng

FRsCS Vol.3 No. 1 (2024)
Official Journal of Dept. of
Chemistry, Federal University of
Dutsin-Ma, Katsina State.
<http://rudmafudma.com>

ISSN (Online): 2705-2362

ISSN (Print): 2705-2354

Theoretical Investigation of Some Anti-*Staphylococcus aureus* Halogenated Hydrazone Derivatives.

^{1*}Mary Ikhaote Ohiole and ²Siaka Abdulfatai

https://doi.org/10.33003/frscs_2024_0301/04

Abstract

Growing incidences of widespread resistance to existing antibiotics are threatening to revert humanity to the pre-antibiotic era where fatality and mortality rates due to bacterial infections were outrageously high. A way out of this public health concern is a deliberate search for novel drug candidates in the drug development pipeline. In this study, a data set of bioactive halogenated hydrazone derivatives was subjected to QSAR modeling using the Genetic Function Approximation technique. Before model building, the compounds were subjected to geometry optimization using the DFT method of Spartan 14 software at the B3LYP level of theory and 6-31G** basis set to obtain their minimum energy geometries. The validated penta-parametric QSAR model ($R^2 = 0.76$, $R^2_{Adj} = 0.70$, $Q^2_{LOO} = 0.63$, $R^2_{Pred} = 0.59$) hinted the predominance of L3m, RDF135s, RDF60m, minHBint7, and ATSC5i descriptors on the observed MIC of the molecules. The validated model predicted the MIC of three newly designed hydrazone analogs; C1, C2, and C3 as 0.0003, 0.0003, and 0.0007 $\mu\text{g/mL}$, respectively. The predicted MIC values of the novel ligands revealed that they possess better potencies than the most potent molecules in the data set. Molecular docking simulations of designed ligands against the active sites of DNA gyrase of the bacterium recorded binding energy values of -8.8, -8.7, and -8.8 kcal/mol, respectively. Furthermore, ADMET profiles of the designed ligands revealed their excellent pharmacokinetic and toxicological profiles. It is envisaged that the wealth of information derived from this work could help in the discovery and development of novel antibiotics against *S. aureus*.

Keywords: Halogenated hydrazone derivatives, *Staphylococcus aureus*, DFT, ADMET, QSAR

Introduction

Pathogenic bacteria constitute a major cause of morbidity and mortality in the human population. These microbes have devised different avenues of evading antibiotics leading to multi-drug resistance, an ugly trend that could overpower the pharmaceutical industry owing to its inability to keep up with the ever-increasing demand for effective novel antibacterial agents (WHO, *et al.*, 2018). Multidrug resistance in pathogenic bacterial species has become so critical that it has been forecasted that by the year 2050, the annual death rate attributable to this ugly scenario could be as high as 10 million (De Kraker *et al.*, 2016). Of particular concern are the rising cases of resistance to existing antibiotics by a Gram-positive bacteria known as *Staphylococcus aureus* (*S. aureus*), a common commensal of the skin that colonizes close to one-third of the human population (Williams *et al.*, 1963). Infections by this bacterial species occur when the skin or mucosal barrier is breached, allowing the organism to penetrate the bloodstream and adjoining tissues. *S. aureus* causes food poisoning, pneumonia, endocarditis, osteomyelitis, sepsis, and toxic shock syndrome (Velasco *et al.*, 2019).

pronounced among the immune-compromised groups such as HIV-positive persons (Hidron *et al.*, 2020).

Treatment of *S. aureus* infections is usually via the use of antibiotics. Regrettably, resistance to these drugs is increasing alarmingly. A major way of mitigating this public health emergency is the search for novel drug candidates in the drug development pipeline. The conventional drug discovery and development approach is a herculean task because of the enormous time and resources expended in the process (Ameji *et al.*, 2017). However, the application of *in silico* techniques as complementary strategies helps to circumvent these bottlenecks. One of these techniques is the application of Quantitative Structure-Activity Relationship (QSAR) modeling. QSAR modeling attempts to analyze statistically, the relationships between the descriptors of molecular structures of congeneric compounds and their observed biological activities (Khatkar *et al.*, 2014; Sahu *et al.*, 2013). Information derived from validated QSAR could be used to optimize the structure of a biologically active ligand for enhanced potency and pharmacokinetic properties (Ameji *et al.*, 2023). An ideal 2D QSAR model takes the form of a regression equation 1.

$$Y = \beta x_1 + \gamma x_2 + \omega x_3 + c \quad \dots\dots\dots (1),$$

where Y is the biological property of concern; x_1 , x_2 , and x_3 are the molecular descriptors; β , γ , and ω are the numerical coefficients; and c is the constant of the regression model. QSAR model plays a significant role in ligand-based drug design because it helps to optimize the potency and drug-like properties of lead compounds (Ameji *et al.*, 2023; Spous *et al.*, 2006). Also, central to modern drug design is the use of molecular docking studies which mimics the binding interaction of small molecules known as ligands with the active sites of a macromolecular target. The magnitude of interaction between a ligand and a target macromolecule is usually

expressed as Gibb's free energy change (ΔG). The lower the magnitude of ΔG of binding, the higher the strength of binding interaction and vice versa (Behl *et al.*, 2021, Hussain *et al.*, 2021). In addition, the safety and ability of a biologically active ligand to exert its requisite pharmacological roles in the biological system is governed by its absorption, distribution, metabolism, excretion, and toxicity (ADMET). *In silico* ADMET profiling is an essential component of modern drug research owing to its ability to minimize attrition rates of drug-like candidates during the preclinical and clinical stages of drug development (Ameji *et al.*, 2022; Daouud *et al.*, 2021).

Hydrazides are chemical compounds derived from the acylation of hydrazine. They are characterized by the presence of nitrogen-to-nitrogen covalent bonds attached to four substituents, with at least one of them being an acyl group. Their significant pharmacological properties have made them components of drugs such as 2-azetidiones (an inhibitor of β -lactamase), Thiazolidinediones (an inhibitor of peptidoglycan synthesis), nifuroxazide (an antibiotic), nifurtimox (an antiameboic), isocarbazide (an antidepressant), iproniazide (anti-tuberculosis), etc (Kumari *et al.*, 2016).

Owing to the enormous therapeutic properties of hydrazide, many *in silico* studies have been carried out on some of its derivatives with the sole aim of obtaining theoretical insights into its biological activities. One such *in silico* investigation is the research work of Mebarka *et al.*, (2021) wherein the authors carried out a combined 3D-QSAR, molecular docking simulation, and ADMET studies on anti-*S. aureus* thienopyrimidine derivatives. Their validated CoMFA and CoMSIA models were used to design some series of novel drug-like compounds.

Khatkar *et al.* (2014) performed QSAR modeling on a series of synthesized p-coumaric acid derivatives. The authors found that the

antimicrobial activities of the compounds were influenced by the molecules' electronic energy, topological parameters, first-order molecular connectivity index, and Wiener index. Also, Cortes et al. (2020) investigated the bioactivity of Twenty-four cannabinoids against Methicillin-Resistant *S. aureus* using QSAR modeling and molecular docking technique. The authors used the validated model to design three new ligands with significant activities against the pathogenic microbes. They also found out that the investigated compounds bind appreciably with penicillin-binding protein and DNA gyrase of the bacterium. Furthermore, Narang et al. (2012) performed multi-target QSAR studies on the antimicrobial properties of nicotinic acid benzylidene hydrazide derivatives. Their validated QSAR model ($R^2 = 0.73$) revealed that the second-order molecular connectivity index descriptor (${}^2\chi$) played the dominant role in the observed antimicrobial properties of the investigated compounds. This study is aimed at the use of QSAR modeling, molecular docking, and ADMET profiling to design potent and non-toxic drug candidates against *S. aureus* from halogenated hydrazide derivatives.

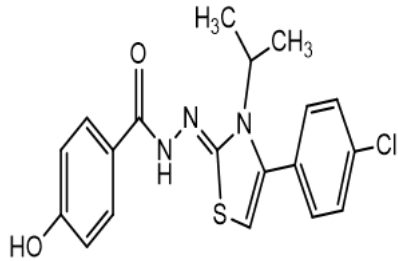
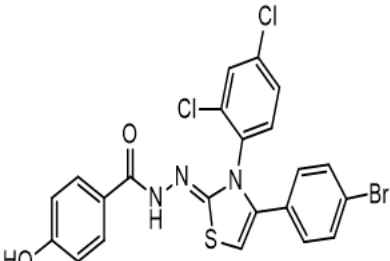
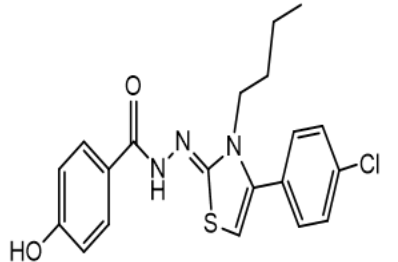
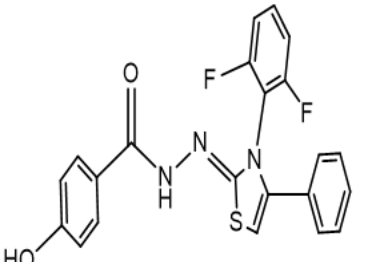
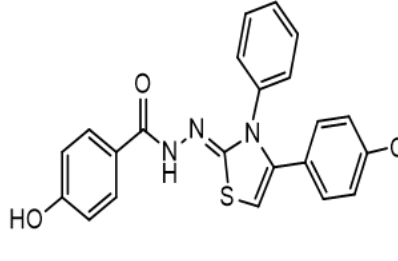
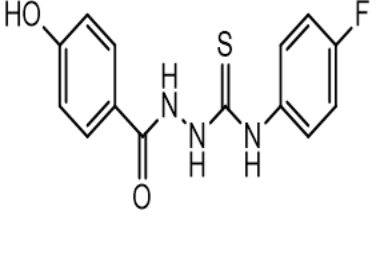
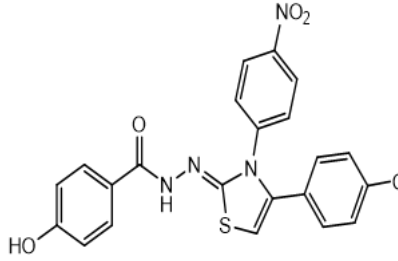
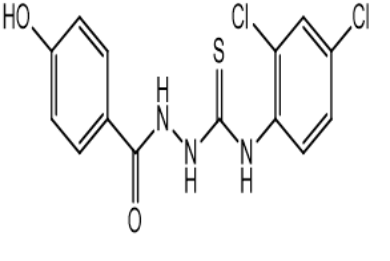
Methods

Collection of Data, Geometry Optimization and Descriptor Calculation

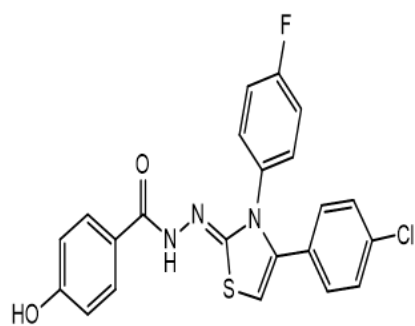
A series of thirty-seven (37) halogenated hydrazide derivatives whose invitro inhibitory activities against *S. aureus* have been established and expressed as minimum inhibitory concentration (MIC) was obtained from literature (Bhole et al., 2020; Ozdemir et al., 2009). The MIC of the compounds was transformed into jMIC (jMIC = log MIC) to get a more linear response and reduce data dispersion in the course of model building (Ameji et al., 2023). Geometry optimization is the process of obtaining the minimum energy conformation of a molecule. ChemDraw Ultra 12.0 was used to draw the 2D structures of the

compounds. These structures were converted into 3D geometry by exporting them sequentially to the Spartan 14 version 1.1.4 software from Wavefunction Inc. The geometry of each of the compounds was optimized using the density functional theory (DFT/B3LYP) approach and the 6-31G* basis set. The descriptors of the optimized structures were calculated with the aid of the PaDEL descriptor tool kit (Ameji et al., 2023; Ameji et al., 2022; Yap, 2011). Table 1 presents the chemical structures and jMIC of the bioactive compounds.

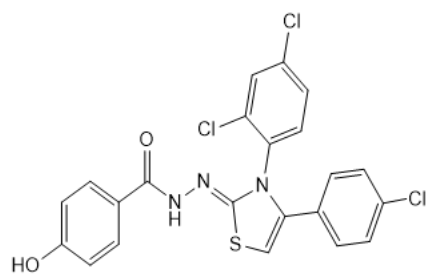
Table 1: Structures and Experimental jMIC values of the Investigated Compounds

S/n	Structure	jMIC ($\mu\text{g/mL}$)	S/n	Structure	jMIC ($\mu\text{g/mL}$)
*1		1.75	20		1.62
2		1.75	21		0.48
3		1.84	22		1.58
4		1.41	23		1.36

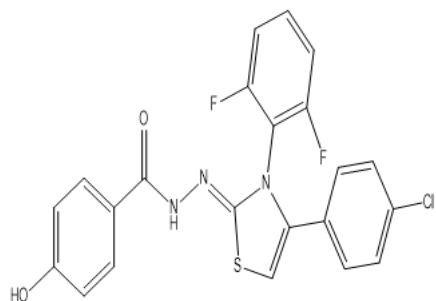
5 1.23



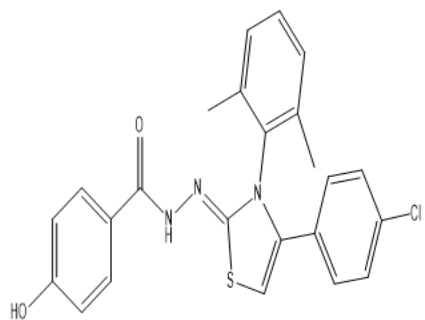
6 1.43



7 1.18

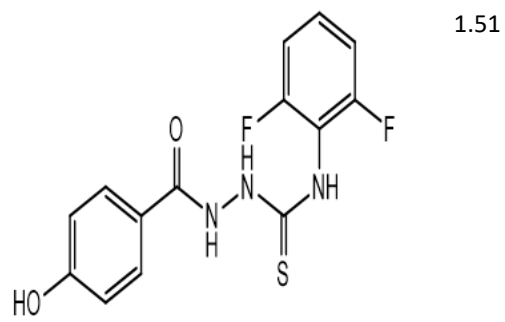


8 1.20

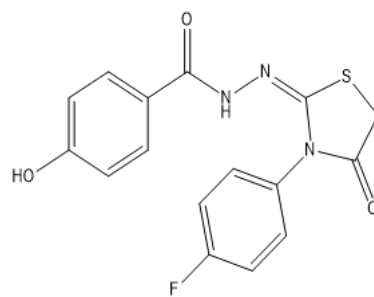


9 1.18

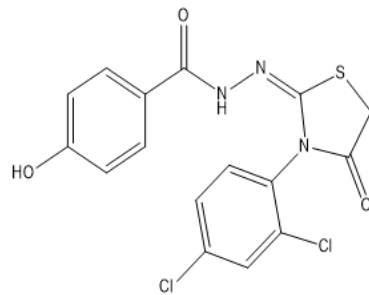
24



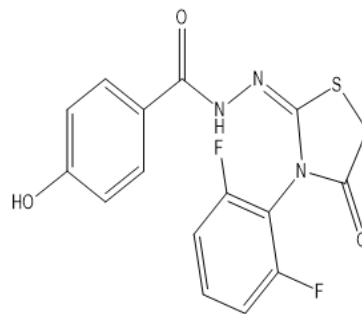
25 1.74



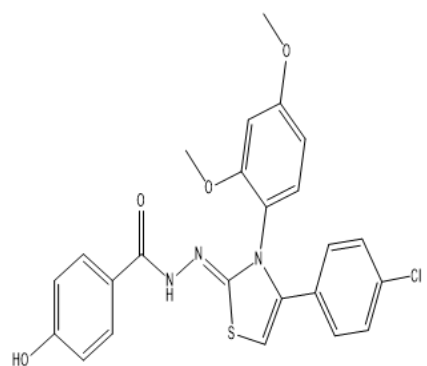
26 0.78



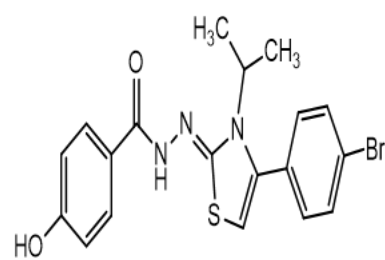
27 1.20



28 1.58

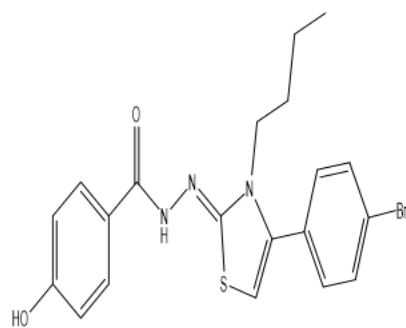


10



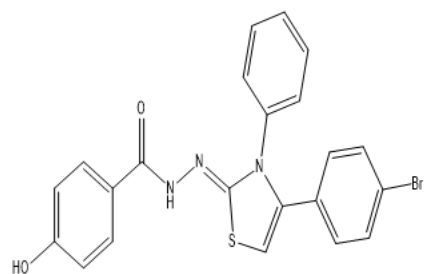
1.43

11



1.77

12

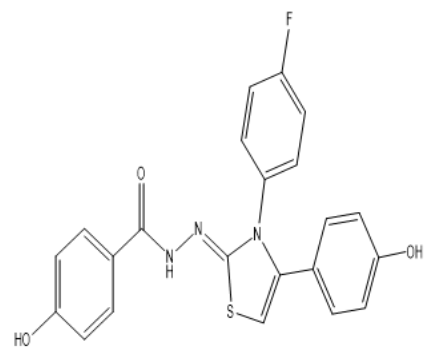


1.75

13

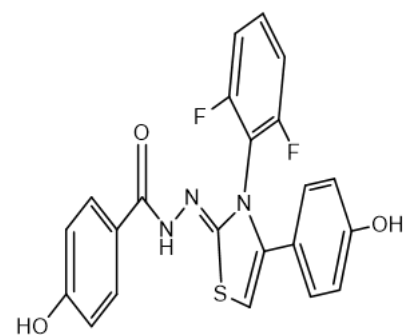
1.90

29



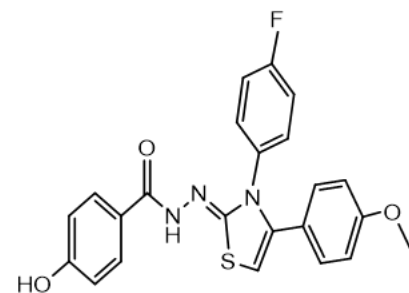
1.36

30



1.51

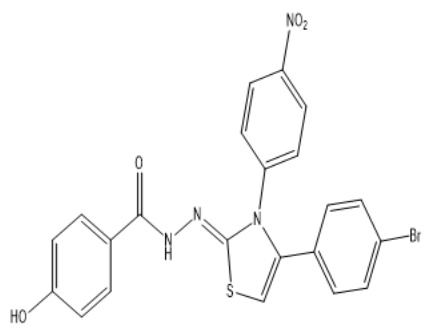
*31



1.74

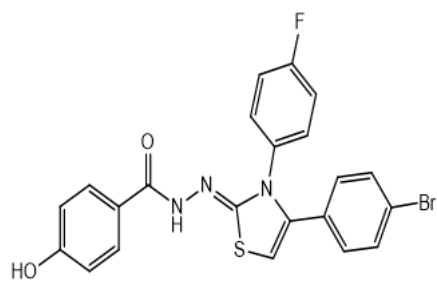
32

0.78



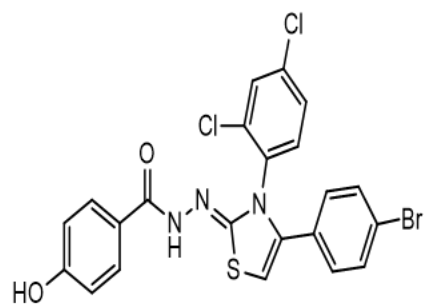
14

1.46



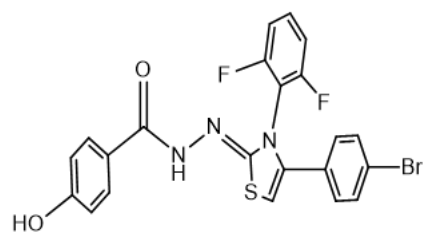
15

0.85



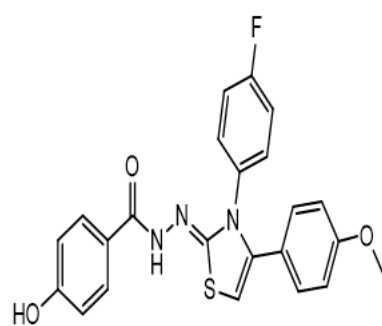
16

1.23



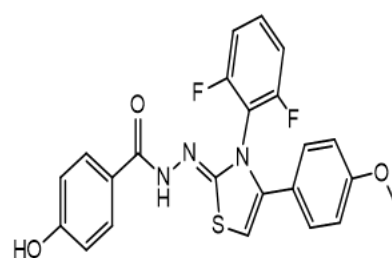
17

1.08



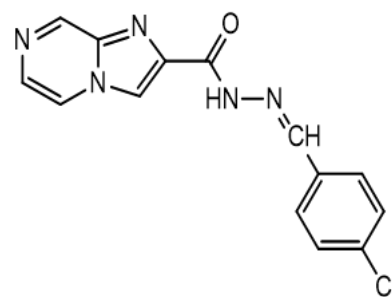
33

1.20



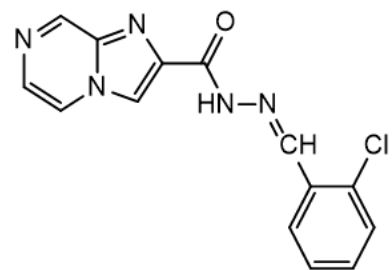
34

1.70



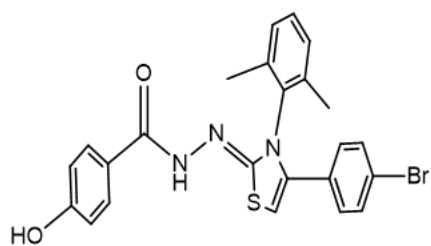
35

2.00



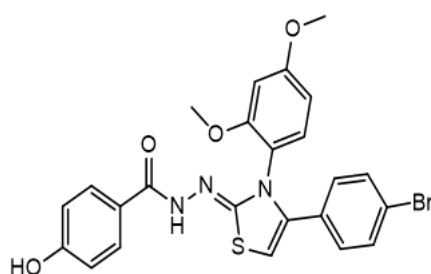
36

2.00



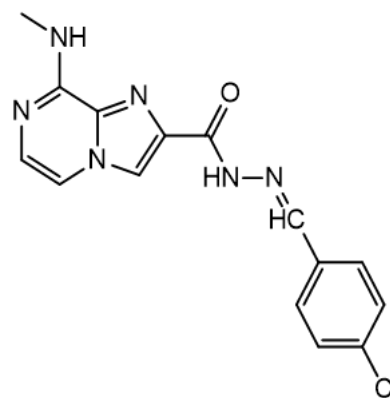
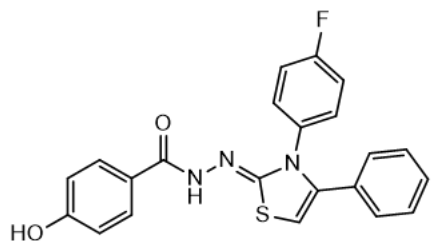
18

1.41



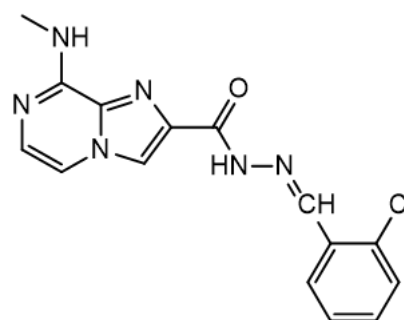
19

1.40



37

2.00



* Statistical Outlier

Building and Validation of QSAR Model

QSAR model was built by splitting the data set of the investigated hydrazide derivatives into a 70% training set and 30% test set using the Data-set-Division GUI V2.1 tool of the DTC laboratory. The training set was used for model building while the test set was used for external validation of the model. The V-WSP data pretreatment tool 1.2v was used to remove redundant descriptors from the calculated pool of descriptors. The Genetic Algorithm v4.1 tool was used to build the optimum QSAR model by setting equation length to 5, mutation probability

was set to 0.3, variance cut off was set to 0.001 and inter-correlation cut off was set to 0.9. The built QSAR model was validated internally using least squares fit (R^2), cross-validated R-squared (Q^2_{LOO}), and adjusted R-squared (R^2_{Adj}). The external prediction ability of the optimum model was adjudged using the predicted R^2 for the external test set (R^2_{Pred}). The validation parameters obtained for the model were compared with standard validation metrics in QSAR modeling (Ameji *et al.*, 2023).

Applicability domain definition

A single QSAR cannot predict the bioactivity of all the molecules in the universe. Thus, it has become necessary to define the chemical space of molecules within its jurisdiction known as its applicability domain (AD). The AD of the optimum QSAR model was defined using the standardization approach of the AD executable jar file in the DTC laboratory.

Variance Inflation Factor Statistics

Statistically, Multicollinearity in multiple linear regression occurs when there exists a high inter-correlation among the independent variables. The Variance Inflation Factor (VIF) statistic was used to check possible multicollinearity among the five descriptors in the model. The Model's VIF was calculated using Equation 2.

$$VIF = \frac{1}{1-R^2} \dots\dots\dots (2),$$

Where R^2 is the correlation coefficient of the multiple regression between the descriptors in the model. A VIF of 1 connotes the complete absence of multicollinearity among the Model's descriptors. Also, a VIF value larger than 10 indicates high instability of the model (30, 31).

Design of New Ligands

To theoretically design more potent analogs of the investigated compounds, the most potent bioactive molecule was selected as a template molecule and subjected to pharmacophoric modifications via the addition of propyl and hydroxyl functional groups around the rings of the template ligand. The geometries of the different derivatives generated were optimized and their descriptors were computed using the aforementioned procedures in section 2.1. Subsequently, the MIC of the designed ligands was predicted using the validated QSAR model. Also, the newly designed ligands were subjected to molecular docking simulation against DNA gyrase, a crucial enzyme of *S. aureus* that plays significant roles during its replication processes (Adeniji *et al.*, 2022, Coba-Male *et al.*, 2022, Jakopin *et al.*, 2017).

Molecular Docking Procedures

The optimized structures of the halogenated hydrazide derivatives (ligands) were prepared on the AutoDock Vina interface and saved in pdbqt file formats. The PDB file of DNA gyrase was retrieved from the protein data bank (www.rcsb.org/pdb) with a PDB code of 5ztj and exported to the Discovery Studio 2016 interface where attached ligands, water molecules, and heteroatoms were removed. The target protein was subsequently exported unto the AutoDock Vina interface where it was further refined via the addition of polar hydrogens and Kollman charges. Also, missing atoms in the protein were checked and repaired. PyRx GUI of AutoDock Vina software was used to perform docking calculations. Visualization of the protein–ligand interactions was done with the aid of Discovery Studio 2016 (Ameji *et al.*, 2023, Adeniji *et al.*, 2022).

Druglikeness and ADMET Profiling

In silico druglikeness evaluation was performed to ascertain the suitability of the therapeutic ligands to be administered as a drug via the oral route. The physicochemical properties of the ligands which define their drug-likeness were computed using the SwissADME online server (www.swissadme.ch/ accessed on 12 May 2023). Lipinski's rule of five and Veber's rule were subsequently used to predict the oral bioavailability of the compounds. Likewise, pharmacokinetic and toxicity prediction was performed on the ligands using the SwissADME (www.swissadme.ch/ accessed on 12 May 2023) and DataWarrior V5.5.0 Chemoinformatics program (Ameji *et al.*, 2023, Ameji *et al.*, 2022).

Results

Model and Statistical Validation

Equation 2 presents the internally and externally validated QSAR model connecting the descriptors of the investigated halogenated hydrazide derivatives and their observed inhibitory activities. The statistical validation parameters of the model as well as the

definitions of the model's descriptors are presented in Tables 2 and 3, respectively. Table 4 gives the Variance Inflation Factor (VIF) statistics of the validated model while the Scatter plot of the model is presented in Figure 1. Furthermore, the plot of experimental jMIC

against predicted jMIC for training and test set molecules are presented in Figures 2 and 3, respectively. Figures 4 and 5 present the residual plot of the model and the significance of the descriptors in the model, respectively.

$$jMIC = 2.3183 - 0.8997 * L3m - 0.0502 * RDF135s - 0.0165 * RDF60m - 0.2595 * minHBint7 + 0.0166 * ATSC5i \dots\dots\dots (3)$$

Table 2: Validation metrics of the QSAR Model

S/n	Parameter	Threshold	Model Value	Statement
1.	Square of Coefficient of determination (R^2)	≥ 0.6	0.76	Excellent
2	Adjusted R-squared ($R^2_{Adj.}$)	≥ 0.6	0.70	Stable
3	Cross-validated R-squared (Q^2_{LOO})	≥ 0.5	0.63	Reliable
4	Predictive R-squared (R^2_{pred})	≥ 0.5	0.59	Robust
5	$R^2 - Q^2_{LOO}$	≤ 0.3	0.13	Stable

Table 3: Description of the Descriptors in the QSAR Model

S/n	Descriptor	Definition	Class
1	L3m	3rd component size directional WHIM index / weighted by relative mass	3D
2	RDF135s	Radial distribution function - 135 / weighted by relative I-state	3D
3	RDF60m	Radial distribution function - 060 / weighted by relative mass	3D
4	minHBint7	Minimum E-State descriptors of strength for potential Hydrogen Bonds of path length 7	2D
5	ATSC5i	Centered Broto-Moreau autocorrelation - lag 5 / weighted by first ionization potential	2D

Table 4: Variance Inflation Factor Statistics

S/n	Descriptor	R^2	VIF
1	L3m	0.55	2.22
2	RDF135s	0.45	1.82
3	RDF60m	0.46	1.85
4	minHBint7	0.32	1.47
5	ATSC5i	0.28	1.39

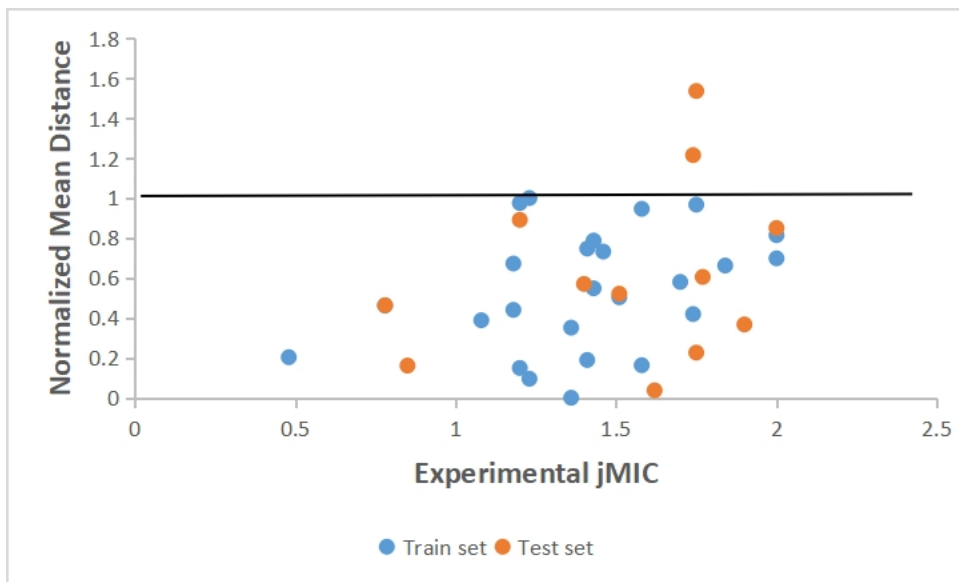


Figure 1: Scatter plot of the Optimum QSAR Model

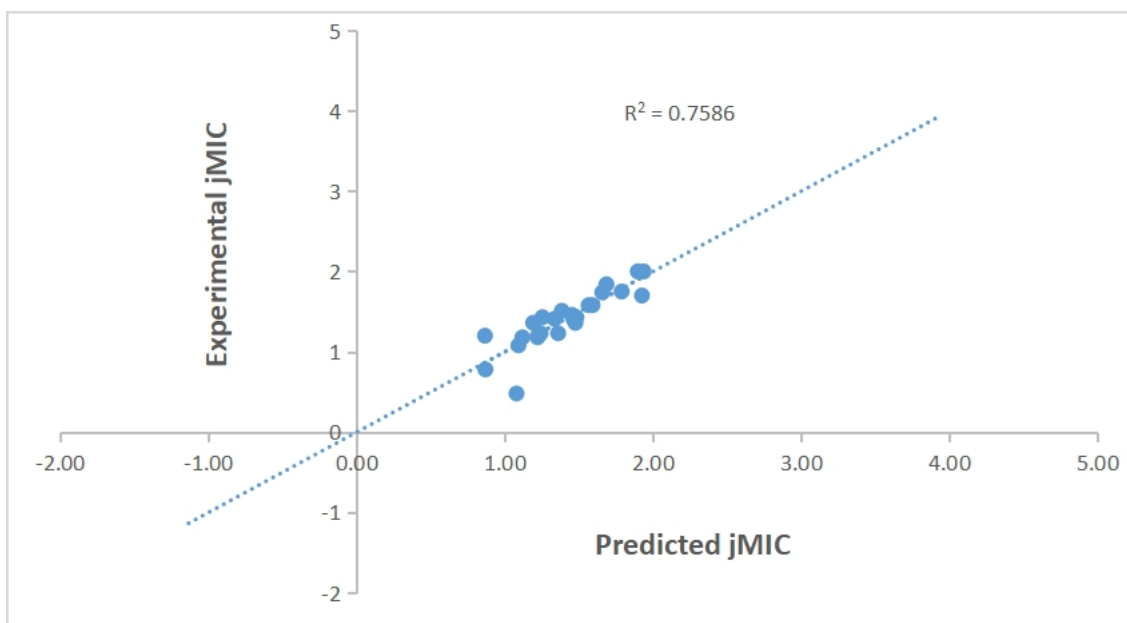


Figure 2: Plot of experimental jMIC against predicted jMIC (training set)

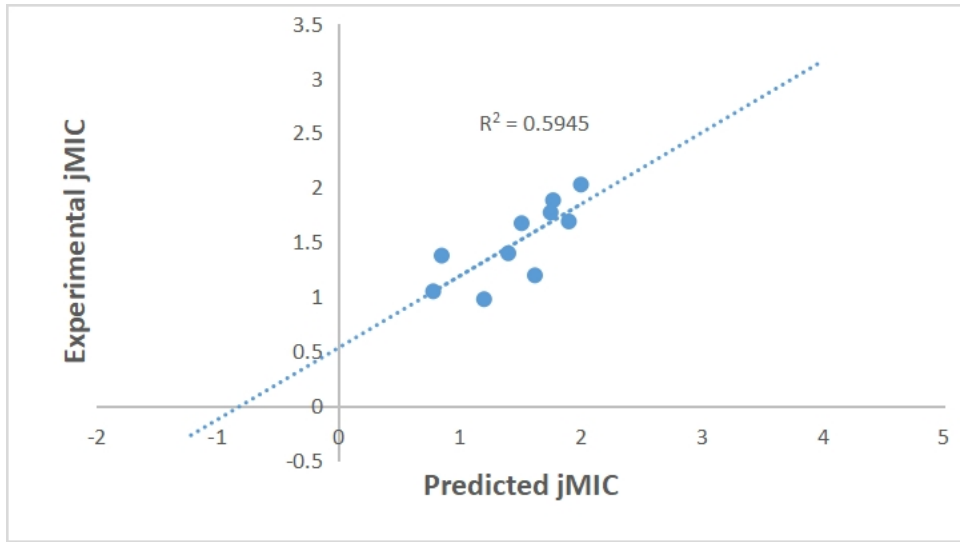


Figure 3: Plot of experimental jMIC against predicted jMIC (test set)

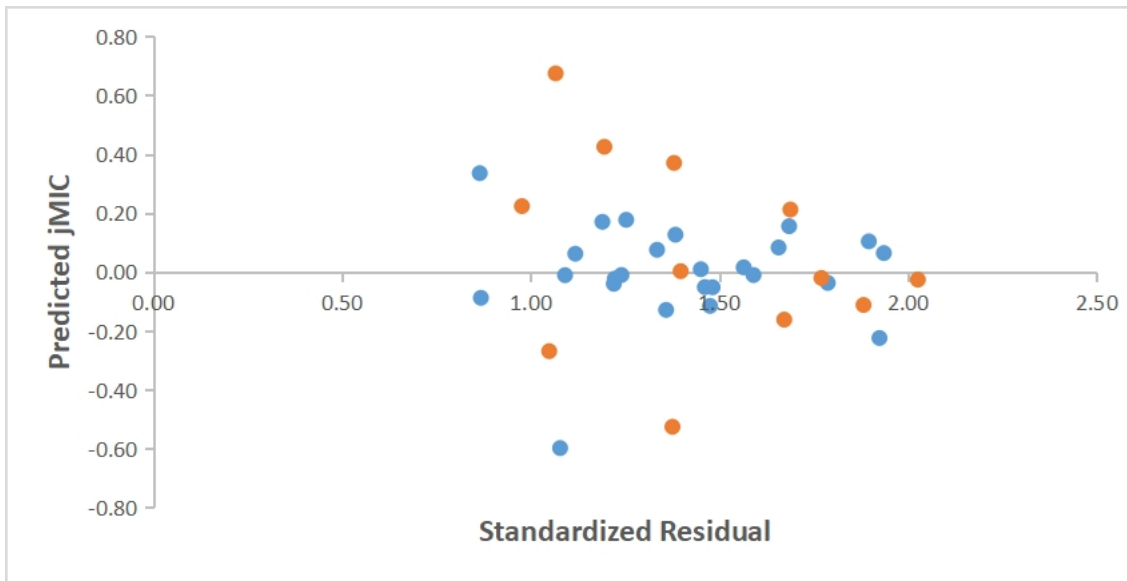


Figure 4: Residual Plot of the validated Model

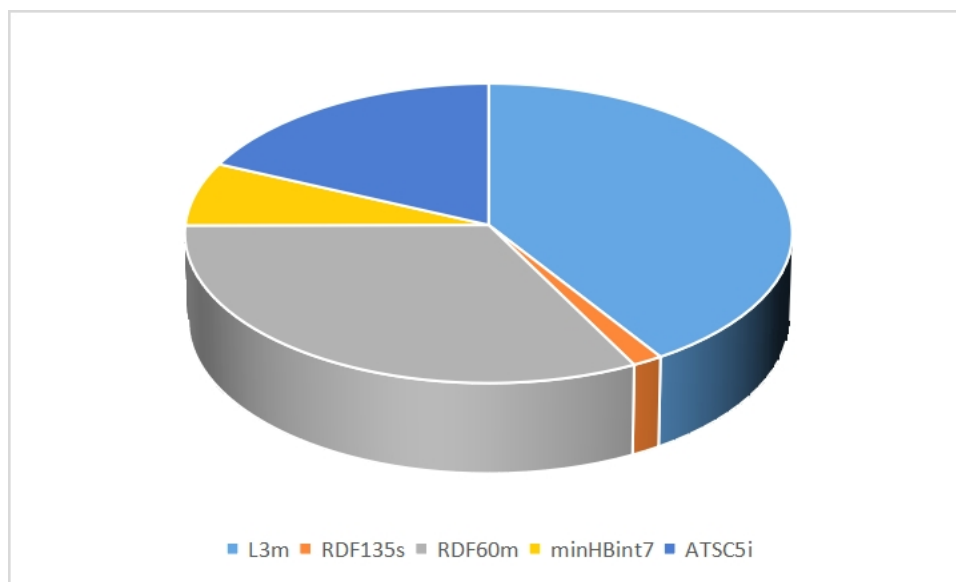


Figure 5: Descriptors' Contribution to the QSAR Model

Newly Designed ligands and their predicted MIC

Figure 6 presents the chemical structures of the newly designed halogenated hydrazide derivatives and a standard inhibitor of DNA gyrase (Ciprofloxacin) of *S. aureus*. The

descriptors of the ligands were calculated using the procedure described in section 2.1 and their MIC was predicted using the generated QSAR model in Equation 3. Table 5 gives the predicted MIC of the novel ligands

Table 5: Predicted MIC of the designed ligand

Ligand	L3m	RDF135s	RDF60m	minHBint7	ATSC5i	pMIC	MIC ($\mu\text{g/mL}$)
C1	0.7365	5.7763	16.4518	0	3.4792	-3.4846	0.0003
C2	0.6704	7.0093	14.4131	0	2.8342	-3.4641	0.0003
C3	0.6729	6.3789	15.6385	-1.0147	3.4792	-3.1809	0.0007

Molecular Docking Simulation Studies

In addition to revealing the binding affinity of ligands against the active sites of target macromolecules, molecular docking also reveals the mechanism of interactions between the

ligand and the receptor. Table 6 presents the binding affinity values of the designed ligands and ciprofloxacin against DNA gyrase while their mechanism of interactions with the receptor is presented in Figure 7.

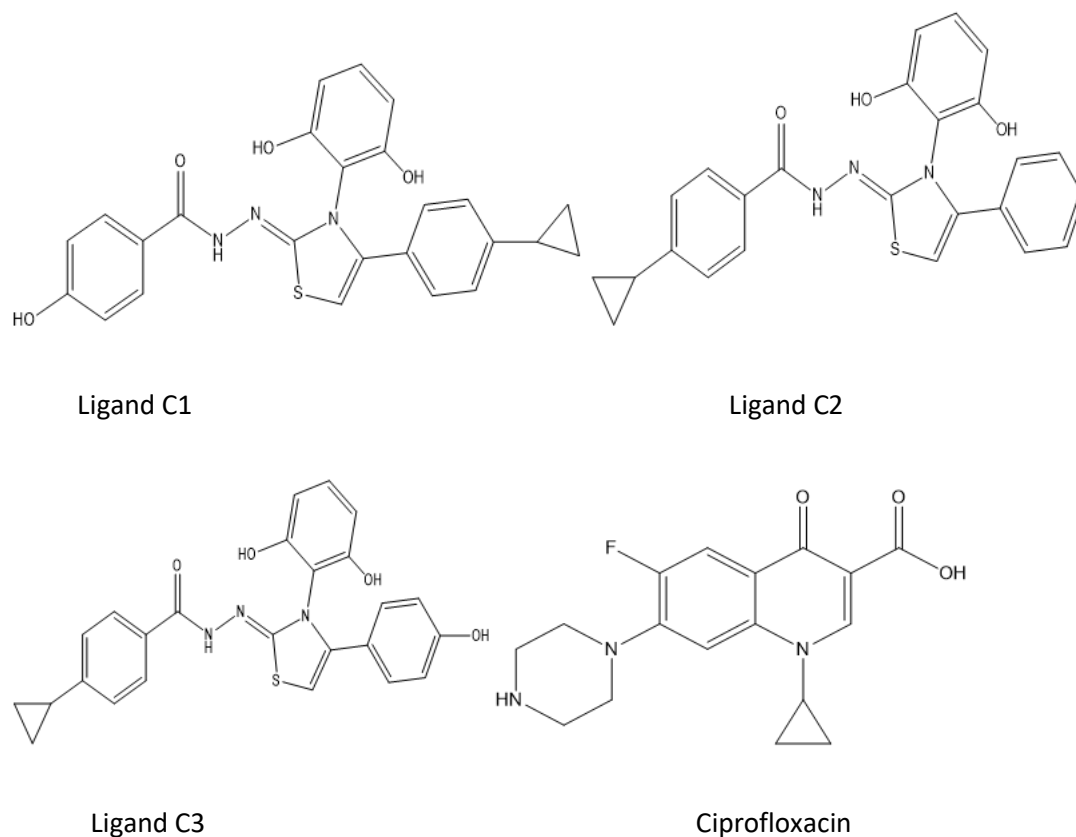
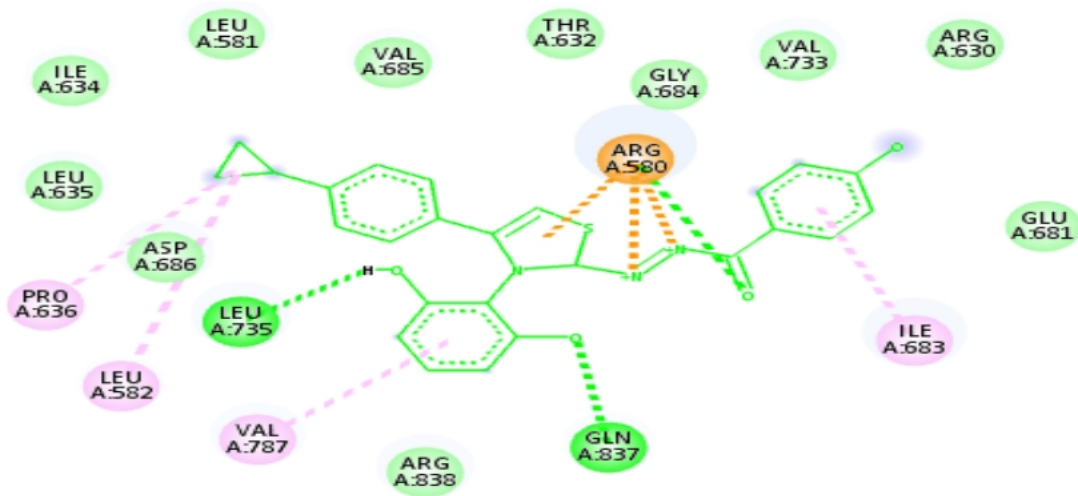


Figure 6: Chemical structures of the novel ligands and Ciprofloxacin

Table 6: The binding affinity values of the ligands against the receptor and major interacting amino acid residues of the macromolecule.

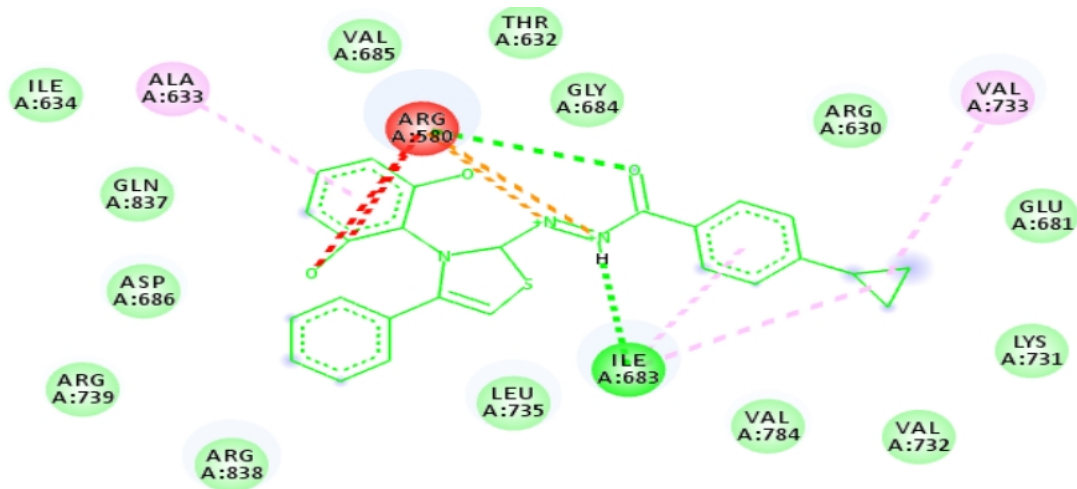
Ligand	ΔG (kcal/mol)	Major interacting amino acid residues
C1	-8.8	ARG 580 (three attractive charges), PRO 636 (an alkyl), LEU 582 (an alkyl), VAL 787 (a pi-alkyl), ILE 683 (a pi-alkyl), ARG 580 (one conventional hydrogen bond), LEU 735 (one conventional hydrogen bond), GLN 837 (one conventional hydrogen bond).
C2	-8.7	ALA 633 (a pi-alkyl), ILE 683 (a pi-alkyl), VAL 733 (an alkyl), ILE 683 (an alkyl), ARG 580 (two unfavorable positive-positive interactions), ARG 580 (two attractive charges), ARG 580 (a conventional hydrogen bond), ILE 683 (a conventional hydrogen bond)
C3	-8.8	ALA 633 (a pi-alkyl), VAL 733 (an alkyl), ILE 683 (an alkyl, a pi-alkyl, and a conventional hydrogen bond), ARG 580 (two attractive charges, an unfavorable positive-positive, a conventional hydrogen bond), ARG 838 (a conventional hydrogen bond), VAL 685 (a conventional hydrogen bond), THR 632 (a conventional hydrogen bond).
Cipro	-7.6	ARG 630 (three alkyl and pi-alkyl), GLN 546 (an amide-pi-stacked), GLU 626 (one carbon-hydrogen), HIS 545 (one carbon-hydrogen), ILE 631 (one conventional hydrogen bond), SER 544 (one conventional hydrogen bond)



Interactions

- | | |
|-------------------------------|------------------------|
| van der Waals | Pi-Cation |
| Attractive Charge | Pi-Donor Hydrogen Bond |
| Conventional Hydrogen Bond | Alkyl |
| Unfavorable Positive-Positive | Pi-Alkyl |

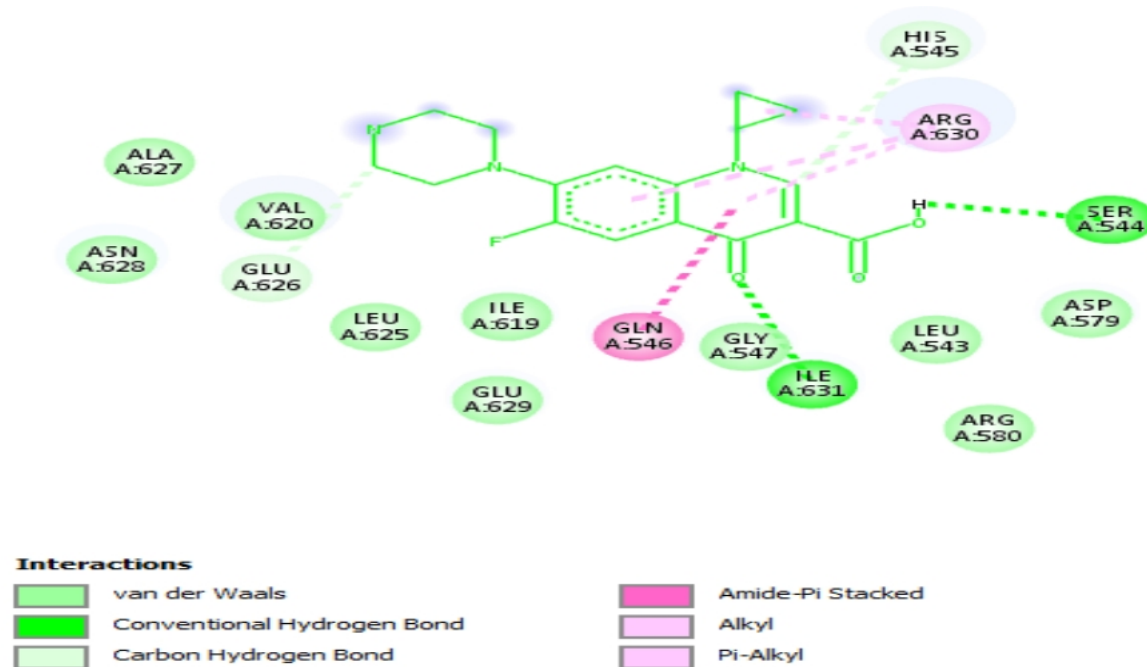
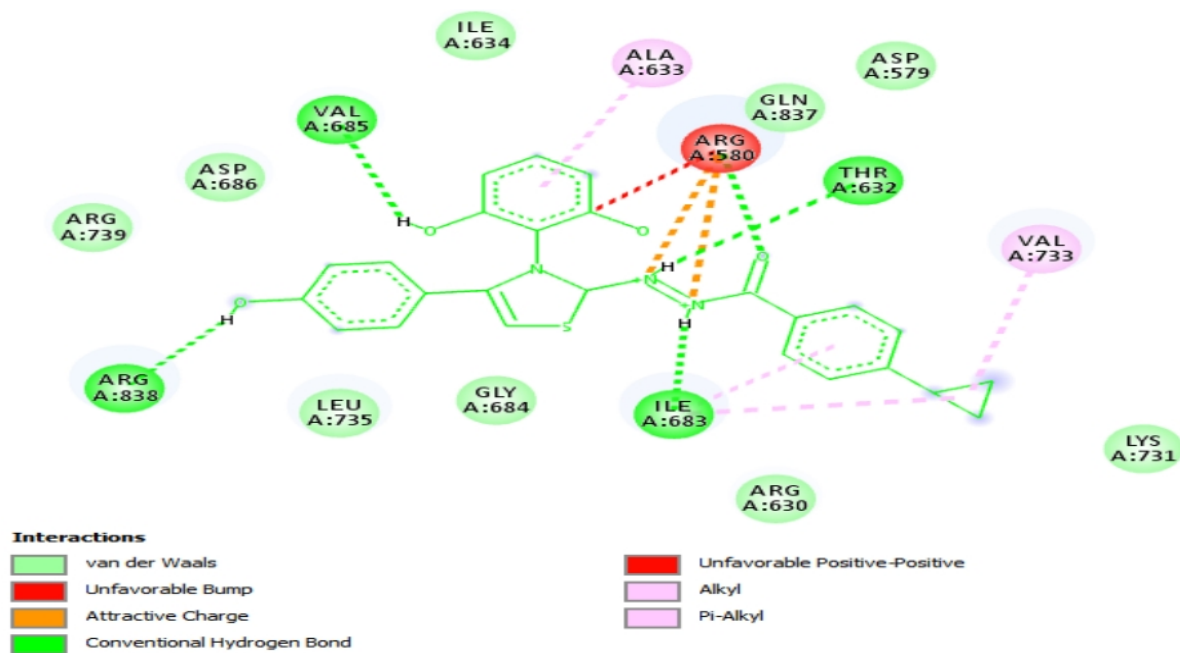
C1/DNA gyrase complex



Interactions

- | | |
|----------------------------|-------------------------------|
| van der Waals | Unfavorable Positive-Positive |
| Unfavorable Bump | Alkyl |
| Attractive Charge | Pi-Alkyl |
| Conventional Hydrogen Bond | |

C2/DNA gyrase complex



Cipro/DNA gyrase complex

Figure 7: Interaction diagram of the ligands with the target

Oral Bioavailability, Pharmacokinetic, and Toxicity Profile of the Ligands

Tables 7 and 8 present the drug-likeness and ADMET profiles of the ligands, respectively.

Table 7: Drug-likeness Profiles of the Ligands

Ligand	C1	C2	C3	Cipro
Rule				
Lipinski's	Yes	Yes	Yes	yes
HBA	5	4	5	5
HBD	4	3	4	2
MW (g mol^{-1})	459.5	443.5	459.5	331.34
cLogP _(o/w)	3.98	4.4	4.0	1.10
Veber's	Yes	Yes	Yes	Yes
NRB	6	6	6	3
TPSA (\AA^2)	135.2	115.1	135.3	74.54

HBA; hydrogen bond acceptor, HBD; hydrogen bond donor, Mw; molecular weight, cLogP; consensus octanol-water partition coefficient, NRB; the number of the rotatable bonds, TPSA; topological polar surface area

Table 8: ADMET profiles of Ligands

	CYP450	GIA	P-gp+	BBB	MUT	TUM	IR	RE	LogK _p
Ligand	Substrate								(cm/s)
C1	Yes	low	No	No	None	None	None	None	-5.6
C2	Yes	High	No	No	None	None	None	None	-5.3
C3	Yes	low	No	No	None	None	None	None	-5.6
Cipro	Yes	High	Yes	No	None	None	None	None	-9.1

ESOL; estimated solubility, GIA; gastrointestinal absorption, BBB; blood-brain barrier penetration, P-gp⁺; P-glycoprotein substrate, MU; mutagenicity, TUM; tumorigenic, IR; irritating effect, RE; reproductive effect

Discussion

Statistical Significance of the Validated QSAR Model

It is a common paradigm in chemistry that the biological activities of congeneric bioactive compounds are a function of their molecular structure. The QSAR model developed to describe the link between the antimicrobial properties of the investigated compounds and their molecular descriptors is given in Equation 2. The comparison of the statistical parameters of the model with the recommended threshold in Table 2 revealed that the model is stable, robust, and possesses excellent predictive power (Adeniji *et al.*, 2022). In addition, the plot of experimental jMIC against the predicted jMIC for training set molecules is presented in Figure

2. The high linearity of the plot further confirms the internal stability of the model. Furthermore, the model was used to predict the jMIC values of an external set of molecules as an additional validation protocol. Figure 3 gives a plot of experimental jMIC against the predicted jMIC for test set molecules. The predictive R² (R²_{pred}) value of 0.59 which is in agreement with the recommended threshold for this parameter (Table 2) implies that the model can predict well the anti-*Staphylococcus aureus* activities of new hydrazide derivatives within its applicability domain. The occurrence of statistical biases in the process of model building has negative implications for the quality of QSAR models. To check for possible biases in the optimum QSAR model, the standardized residuals were plotted

against the predicted jMIC values (Figure 4). The propagation of residuals on both sides of the zero lines confirms the absence of systematic error in the model development (Ameji *et al.*, 2023). In multiple linear regression, orthogonality connotes that the dependent variables are genuinely independent. This is an essential requirement of a robust and statistically significant QSAR model. The VIF statistics on the descriptors of the optimum QSAR model (Table 4) reveal that all the descriptors possess VIF values of less than 10. Thus, they are all reasonably orthogonal.

Outliers are data points that display significant deviation from other observations. The presence of an outlier in the data set of molecules used for QSAR modeling reduces the statistical quality of the model. An outlier analysis performed on the built QSAR model revealed the presence of two outliers (Figure 1). As a way of ensuring a quality model, these data points were expunged from the data set.

Descriptors' Significance

The biological properties of molecules are strongly linked to the descriptors of their molecular structures. The QSAR model developed to harness the dominant descriptors of the observed anti-*Staphylococcus aureus* of the halogenated hydrazide derivatives revealed the dominant influence of L3m, RDF135s, RDF60m, minHBint7, and ATSC5i descriptors. The analysis of the descriptors' contribution presented in Figure 5 revealed that RDF60m and L3m descriptors played dominant roles in the observed inhibitory activities of the investigated hydrazide derivatives. The negative coefficients of both descriptors as revealed by the model show that the MIC of the compounds varies inversely with the values of these descriptors and vice versa. Thus, the lower the values of these descriptors in a molecule, the higher its MIC against *S. aureus* and vice versa. Since potency varies inversely with MIC, increased values of RDF60m and L3m descriptors in

halogenated hydrazides could improve their inhibitory role against the growth of *Staphylococcus aureus*.

Predicted MIC of the Designed Ligands

Ligand 21 possesses the best potency *in vitro*. It was selected as a template for designing more potent analogs; C1, C2, and C3 (Figure 6). The developed QSAR model predicts the MIC values of C1, C2, and C3 as 0.0003 $\mu\text{g/mL}$, 0.0003 $\mu\text{g/mL}$, and 0.0007 $\mu\text{g/mL}$, respectively (Table 5). The designed ligands were found to possess more potency when compared with the template molecule with a MIC value of 3.0 $\mu\text{g/mL}$.

Molecular Docking Investigation

Table 6 presents the results of molecular docking simulations and mechanisms of interaction of C1, C2, C3, and Ciprofloxacin with the target DNA gyrase. C1, C2, C3, and Ciprofloxacin bind to the active sites of the receptor with Gibb's free of binding value of -8.8, -8.7, -8.8, and -7.6 kcal/mol, respectively. The designed ligands were found to bind more strongly to the macromolecule when compared to the standard inhibitor of DNA gyrase (Ciprofloxacin). Analysis of the mode of interaction of the ligands with the active sites of DNA gyrase shown in Figure 7 revealed that C1 binds to the receptor via; the formation of three attractive charges with ARG 580; an alkyl interaction with PRO 636; an alkyl interaction with LEU 582; two pi-alkyl bonds with VAL 787 and ILE 683; and three conventional hydrogen bonds with LEU 735, ARG 580, and GLN 837 amino acid residues of DNA gyrase. Furthermore, ligand C2 forms: two pi-alkyl bonds with ALA 633 and ILE 683; two alkyl interactions with VAL 733 and ILE 683; two unfavorable positive-positive interactions with ARG 580 and two conventional hydrogen bonds with ARG 580 and ILE 683. Also, ligand C3 binds to the active sites of the target macromolecule via the formation of two pi-alkyl bonds with ALA 633 and ILE 683; two alkyl interactions with VAL 733 and ILE 683; two

attractive charges and unfavorable positive-positive interactions with ARG 580; and five conventional hydrogen bond with ARG 580, ARG 838, ILE 683, VAL 685, and THR 632 amino acid residues of the target protein. The reference ligand on the other hand binds to the binding pocket of DNA gyrase through the formation of three alkyl and pi-alkyl with ARG 630; an amide-pi-stacked bond with GLN 546; one carbon-hydrogen bond with GLU 626; one carbon-hydrogen interaction with HIS 545; and two conventional hydrogen bonds with ILE 631 and SER 544 amino acid residues. The reference ligand binds to the target via a mechanism that is different from the designed ligands.

Oral bioavailability Assessment

Most drugs designed for systemic effects are administered conveniently via the oral route (Azma *et al.*, 2022). Hence, the evaluation of the oral bioavailability of therapeutic compounds is a cardinal aspect of modern drug discovery. Lipinski's rule of five and the Veber rule were used for predicting this important parameter in the investigated bioactive ligands. According to Lipinski's rule, an orally bioavailable drug must not violate more than one of the following rules; $Mw \leq 500$, $nHBD \leq 5$, $Log P \leq 5$, and $nHBA \leq 10$. Veber's rule on the other hand states that an orally bioavailable drug must have $nNRB$ that is less than 10 and $TPSA$ that is less than 140 \AA^2 (Ameji *et al.*, 2023). The oral bioavailability profile of the ligands presented in Table 7 reveals that they obey both rules, an indication of their positive drug-likeness.

Assessment of Pharmacokinetic and Toxicity Profiles of the Ligands

Pharmacokinetics is primarily concerned with the mode of interaction of the body with administered therapeutic compounds for the entire duration of exposure with particular reference to their absorption, distribution, metabolism, and excretion of the compounds. The ability of a therapeutic compound to go through intestinal absorption before distribution

to the proposed target site where it can elicit its pharmacological effects is an important component of pharmacokinetics investigation (Cardenas *et al.*, 2017). The ADME profile of the ligands (Table 8) reveals that C2 has a similar gastrointestinal absorption potential as Ciprofloxacin. Both possess high gastrointestinal absorption. C1 and C3 both have low gastrointestinal absorption.

An important pharmacokinetic investigation is the oxidative biotransformation of therapeutic ligands in the biological system. This fundamental role is catalyzed by the cytochromes P450 group of enzymes (CYP450). A Ligand that is non-substrate of CYP450 could pose adverse health effects to the body due to its slow or poor metabolism. The ADME data (Table 8) of the ligands reveals that the designed ligands are all substrates of CYP450, just like the standard antibiotic, and as such could be easily metabolized by CYP450 enzymes.

Blood-brain barrier (BBB) is a monolayer of endothelial cells between the blood and the central nervous system (CNS) that controls the entry of chemical substances from the blood to the brain (Abbot *et al.*, 2010), creating a stable microenvironment for optimum neuronal function to avert acute CNS damage. The predicted BBB penetration potential of the designed ligands (Table 8) shows that they are non-permeant of the endothelial cell and as such may pose no threat to the CNS.

Permeability glycoprotein (P-gp) are membrane-embedded proteins in the gastrointestinal tract, BBB, liver, kidney, and placenta that eliminate harmful chemicals from the biological system through its efflux action (Chen *et al.*, 2018) Unlike the standard antibiotic, all the designed ligands are found to be non-substrate of P-gp (Table 8). It could be inferred that their pharmacokinetics profiles may be unaffected by the efflux action of P-gp. Another important pharmacokinetic parameter worthy of consideration especially for therapeutic

compounds that require transdermal administration is the skin permeability (LogKp). The LogKp data of the investigated ligands presented in Table 8 revealed that all the compounds, just like the standard reference antibiotic, have poor skin penetration potentials due to the negative values of their LogKp (Khan *et al.*, 2017). Additionally, the toxicity profiles (Table 8) of the compounds revealed that none of them is mutagenic, tumorigenic, irritating, or pose any adverse effect on the reproductive system.

Conclusion

Rising cases of multidrug resistance in *Staphylococcus aureus* are a major threat to public health. In addition to the misuse of antibiotics in human and veterinary settings, dwindling research in antibiotic drug discovery and development contributed enormously to this public health emergency. A way out of this quagmire is a deliberate search for novel drug candidates in the drug discovery and development pipeline. In this, a set of bioactive halogenated hydrazide derivatives were subjected to QSAR modeling to find the mathematical link between their structures and their observed antibiotic properties against *Staphylococcus aureus*. The validated model was used to design more potent novel analogs of the compounds. The designed ligands were further subjected to molecular docking simulation against the active sites of DNA gyrase target of the bacteria species to get insights into the mechanism of action of the ligands at the atomic and molecular level. The ligands were found to bind strongly to the target via hydrophobic, electrostatic, and conventional hydrogen bond formation. Also, ADMET profiling of the bioactive ligands revealed their sound oral bioavailability, and excellent pharmacokinetic and toxicity profiles. However, this is an *insilico* investigation, and as such *invitro* and *in vivo* investigations are required to validate the findings of this research.

References

- Abbott, N. J., Patabendige, A. A. K., Dolman, D. E. M., Yusof, S. R., and Begley, D. J. (2010). Structure and function of the blood-brain barrier. *Neurobiol. Dis.* 37, 13–25. doi: 10.1016/j.nbd.2009.07.030
- Adeniji SE, Ajala A, Arthur DE, Abdullahi M, Areguamen OI (2022). Chemometric Study, Homology Modeling of G Protein-Coupled Bile Acids Receptor (GPBAR_HUMAN) of Type-2 Diabetes Mellitus, Virtual Screening Evaluation, Drug-Likeness and ADME Prediction for Newly Designed Compounds, *Macromolecular research*, 1-19, DOI 10.1007/s13233-022-0071-3
- Adeniji SE, Ajala A, Arthur DE, Abdullahi M, Areguamen OI (2022). Chemometric Study, Homology Modeling of G Protein-Coupled Bile Acids Receptor (GPBAR_HUMAN) of Type-2 Diabetes Mellitus, Virtual Screening Evaluation, Drug-Likeness and ADME Prediction for Newly Designed Compounds, *Macromolecular research*, 1-19, DOI 10.1007/s13233-022-0071-3
- Ameji J.P, Muhammad IS, Akinleye SR, Okorn GA, Aderemi W.I. (2017). *Insilico* predictive model for anti-microbial properties of Ni (II)-Schiff bases' complexes against *Staphylococcus aureus* and *Candida albicans*. *Int J Biochem Biophys Mol Biol* 2: 36e46. <https://doi.org/10.11648/j.ijbbmb.2017.0205.11>.
- Ameji, J.P., Uzairu, U., Shallangwa, G.A., Uba, S., (2022). Virtual screening of novel pyridine derivatives as effective inhibitors of DNA gyrase (GyrA) of salmonella typhi, *Current Chemistry Letters*. 12, 1–16. DOI: [10.5267/j.ccl.2022.10.002](https://doi.org/10.5267/j.ccl.2022.10.002)
- Ameji JP, Uzairu A, Shallangwa GA, Uba S (2023). Obstructing *Salmonella typhi*'s virulence in eukaryotic cells through design of its SipB protein antagonists. *Journal of Taibah University Medical Sciences* (2023) 18(4), 726e736
- Azman, M.; Sabri, A.H.; Anjani, Q.K.; Mustaffa, M.F.; Hamid, K.A. (2022). Intestinal Absorption Study: Challenges and Absorption Enhancement Strategies in Improving Oral Drug

- Delivery. *Pharmaceuticals*, 15, 975. <https://doi.org/10.3390/ph15080975>
- Behl T, Kaur I, Sehgal A, Singh S, Bhatia S, Al-Harrasi A, *et al.*, (2021) Bioinformatics Accelerates the Major Tetrad: A Real Boost for the Pharmaceutical Industry. *IJMS* 22:1-28
- Bhole PR, Bhusari PK (2010). Synthesis and 3D-QSAR of p-Hydroxybenzohydrazide Derivatives With Antimicrobial Activity Against Multidrug-Resistant *Staphylococcus aureus* Article. *Journal of the Korean Chemical Society*. 54 (1): 77-87. DOI: 10.5012/jkcs.2010.54.01.077
- Cárdenas, P.A.; Kratz, J.M.; Hernández, A.; Costa, G.; Ospina, L.F.; Baena, Y.; Simões, C.M.O.; Jimenez-Kairuz, Á.; Aragon, M. (2017). In vitro intestinal permeability studies, pharmacokinetics and tissue distribution of 6-methylcoumarin after oral and intraperitoneal administration in Wistar rats. *Braz. J. Pharm. Sci.*, 53
- Chen C, Lee M, Weng C; Leong MK (2018). Theoretical Prediction of the Complex P-Glycoprotein Substrate Efflux Based on the Novel Hierarchical Support Vector Regression Scheme. *Molecules* 2018, 23, 1820; doi:10.3390/molecules23071820
- Coba-Males MA, Santamaría-Aguirre J, Alcívar-León CD. In Silico Evaluation of New Fluoroquinolones as Possible Inhibitors of Bacterial Gyrases in Resistant Gram-Negative Pathogens. *Chem. Proc*, 8, 43, 2022, <https://doi.org/10.3390/ecsoc-25-11753>
- Cortes E, Mora J, Márquez E (2020). Modelling the Anti-Methicillin-Resistant *Staphylococcus aureus* (MRSA) Activity of Cannabinoids: A QSAR and Docking Study. *Crystals* 2020, 10, 692; doi:10.3390/cryst10080692
- De Kraker, M.E.A.; Stewardson, A.J.; Harbarth, S., Will. (2016). 10 Million People Die a Year due to Antimicrobial Resistance by 2050? *PLoS Med.*, 13: e1002184
- Daoud, N.E.K., Deb, P.K., Alzweiri, M., Borah, P., Venugopala, K.N., Hourani, W., *et al.*, (2021). ADMET profiling in drug discovery and development: perspectives of in silico, in vitro and integrated approaches. *Curr Drug Metab.* <https://doi.org/10.2174/1389200222666210705122913>
- Ejeh S, Uzairu A, Shallangwa GA, Abechi SE, Ibrahim MT (2022). In silico design and pharmacokinetics investigation of some novel hepatitis C virus NS5B inhibitors: pharmacoinformatics approach, *Bulletin of the National Research Centre* 46; 109 <https://doi.org/10.1186/s42269-022-00796-y>
- Erickson, M. A., and Banks, W. A. (2018). Neuroimmune axes of the bloodbrain barriers and blood-brain interfaces: bases for physiological regulation, disease states, and pharmacological interventions. *Pharmacol. Rev.* 70, 278–314. doi: 10.1124/pr.117.014647
- Gramatica P. (2013). On the development and validation of QSAR models. *Methods Mol Biol*, 930:499-526 doi: 10.1007/978-1-62703-059-5_21
- Hidron, A.; Moanna, M.D.A.; Russell Kempker, M.D.; David Rimland, M.D. (2010). Methicillin-resistant *Staphylococcus aureus* in HIV-infected patients. *Infect. Drug Resist.* 73, 73–86.
- Hussain W, Rasool N, Khan YD (2021). Insights into Machine Learning-based approaches for Virtual Screening in Drug Discovery: Existing strategies and streamlining through FP-CADD. *Current Drug Discovery Technologies* 18: 463–72
- Jaiswal, M., Khadikar, P.V., Scozzafava, A., Supuran, C.T., (2004). Carbonic anhydrase inhibitors: the first QSAR study on inhibition of tumor-associated isoenzyme IX with aromatic and heterocyclic sulfonamides. *Bioorg. Med. Chem. Lett.* 14, 3283–3290.
- Jakopin Z, Ilas J, Barancokova J, *et al.* (2017). Discovery of substituted oxadiazoles as a novel scaffold for DNA gyrase inhibitors, *European Journal of Medicinal Chemistry*, 130: 171–184, 2017

- Khatkar A, Nanda A, Kumar P, Narasimhan B (2014). Synthesis, antimicrobial evaluation and QSAR studies of p-coumaric acid derivatives. *Arabian Journal of Chemistry*, <http://dx.doi.org/10.1016/j.arabjc.2014.05.018>
- Khatkar A, Nanda A, Kumar P, Narasimhan B (2014). Synthesis, antimicrobial evaluation and QSAR studies of p-coumaric acid derivatives. *Arabian Journal of Chemistry*. <http://dx.doi.org/10.1016/j.arabjc.2014.05.018>
- Khan MF, Bari MA, Islam MK, Islam MS, Kayser MS, Nahar N, Al-Faruk M, Rashid MA. (2017). The natural anti-tubercular agents: In silico study of physicochemical, pharmacokinetic and toxicological properties. *J App Pharm Sci.*;7:034-8
- Kumari M., Narang R. (2016). Structure activity relationship and mechanism of action of hydrazide derivatives as antimicrobial molecule. *J Chem Pharmaceut Res*, 8, 823-836.
- Lippmann, E. S., Al-Ahmad, A., Palecek, S. P., and Shusta, E. V. (2013). Modeling the blood-brain barrier using stem cell sources. *Fluids Barriers CNS* 10:2. doi: 10.1186/2045-8118-10-2
- Mebarka O, Belaidi S, Khamouli S, Belaidi H, Chtita S (2021). Combined 3D-QSAR and Molecular Docking Analysis of Thienopyrimidine Derivatives as *Staphylococcus aureus* Inhibitors. *Acta Chimica Slovenica* 68(2). DOI: [10.17344/acsi.2020.5985](https://doi.org/10.17344/acsi.2020.5985)
- Narang R, Narasimhan B, Sharma S, Sriram D, Yogeewari P, De Clercq E, Pannecouque C, Balzarini J (2012). Synthesis, antimycobacterial, antiviral, antimicrobial activities, and QSAR studies of nicotinic acid benzylidene hydrazide derivatives. *Med Chem Res* (2012) 21:1557–1576. DOI 10.1007/s00044-011-9664-7
- Ozdemir A, Turan-Zitouni G, Kaplancikli AZ, Tunali Y (2009). Synthesis and biological activities of new hydrazide derivatives. *Journal of Enzyme Inhibition and Medicinal Chemistry*, 24(3): 825–831. DOI: 10.1080/14756360802399712
- Sahu, V., Sharma, P., Kumar, A., (2013). Synthesis and QSAR modeling of 1-[3-methyl-2-(aryldiazenyl)-2H-aziridin-2-yl]ethanones as potential antibacterial agents. *Med. Chem. Res.* 22 (5), 2476–2485.
- Sakr, A.; Brégeon, F.; Mège, J.L.; Rolain, J.M.; Blin, O. (2018) *Staphylococcus aureus* nasal colonization: An update on mechanisms, epidemiology, risk factors, and subsequent infections. *Front. Microbiol.* 9, 2419.
- Shapiro, S., Bernhard, G. (1998). Inhibition of Oral Bacteria by Phenolic Compounds; QSAR Analysis using Molecular Connectivity. *Molecular informatics*, 17 (4): 327-337.
- Sproun DG, Zhang J, Zhang L, Wang Z, Tepper MA. (2006). Kinase inhibitor recognition by use of a multivariable QSAR model. *J Mol Graph Model* 24(4): 278e295. <https://doi.org/10.1016/j.jmgm.2005.09.004>.
- Trott O, Olson AJ (2010). AutoDock Vina: improving the speed and accuracy of docking with a new scoring function, efficient optimization, and multithreading, *Journal of Computational Chemistry*, 31, 455-61. doi: 10.1002/jcc.21334
- Velasco, V.; Quezada-Aguiluz, M.; Bello-Toledo, H. (2019). *Staphylococcus aureus* in the Meat Supply Chain: Detection Methods, Antimicrobial Resistance, and Virulence Factors. In *Staphylococcus and Streptococcus*; Kirmusaoğlu, S., Ed.; IntechOpen: Rijeka, Croatia,.
- Wertheim, H.F.L.; Melles, D.C.; Vos, M.C.; van Leeuwen, W.; van Belkum, A.; Verbrugh, H.A.; Nouwen, J.L. (2005). The role of nasal carriage in *Staphylococcus aureus* infections. *Lancet Infect. Dis.* 5, 751–762.
- Wilhelm, I., and Krizbai, I. A. (2014). In vitro models of the blood-brain barrier for the study of drug delivery to the brain. *Mol. Pharm.* 11, 1949–1963. doi: 10.1021/mp500046f
- Williams, R.E. (1963) Healthy carriage of *Staphylococcus aureus*: Its prevalence and importance. *Bacteriol. Rev.*, 27, 56–71.

World Health Organization (WHO). (2018). Fact Sheet. Available online: <https://www.who.int/news-room/fact-sheets/detail/antibiotic-resistance> (accessed on 20 September 2022).

Yap CW. (2011). PaDEL-descriptor: an open source software to calculate molecular descriptors and fingerprints. *J Comput Chem*; 32(7): 1466e1474.

Zakari YI, Uzairu A, Shallangwa GA, Abechi SE. (2021). Molecular modelling and design of some β -amino alcohol grafted 1,4,5-trisubstituted 1,2,3-triazoles derivatives against chloroquine sensitive, 3D7 strain of *Plasmodium falciparum*, *Heliyon* 7:e05924.